Letter

Electrode engineering for improving resistive switching performance in single crystalline CeO$_2$ thin films

Zhaoliang Liao [a,b,*], Peng Gao [a], Yang Meng [a], Wangyang Fu [a], Xuedong Bai [a], Hongwu Zhao [a], Dongmin Chen [a,*]

[a] Beijing National Laboratory for Condensed Matter Physics, Institute of Physics, Chinese Academy of Sciences, Beijing 100190, China
[b] Department of Physics and Astronomy, Louisiana State University, Baton Rouge, LA 70810, USA

ARTICLE INFO

ABSTRACT

We have studied the electrode effect on the resistive switching behavior in the single crystalline films of CeO$_2$ grown on Nb–SrTiO$_3$. The fabricated devices with the top electrode made of non-reactive metals (Ag, Au, Pt) show bipolar resistive switching but are volatile. In contrast, the devices with top electrodes made of reactive metals (Al, Ta, Ti) present different bipolar resistive switching direction and are non-volatile, with Ta one having the best in OFF/ON switching ratio. The devices with these kinds of electrodes also exhibit remarkably different rectification behavior because of the difference of electrode/CeO$_2$ interface formation. These results demonstrate that it is possible to improve the performance of resistive switching by electrode engineering.

1. Introduction

Resistive switching (RS) in simple Metal/Metal-Oxide/Metal sandwiched structure has attracted a great interest in both the industry and the materials science community recently [1–3]. Resistance in such structured devices can be varied by the application of external electric field and integrated into the high density and high speed resistance random access memory (RRAM) [4], which shows a promising candidate for the next generation of memory devices. Many experiments have demonstrated that the properties of electrodes could effectively affect the devices' functionality. It is found that non-polar and bipolar RS in TiO$_2$ thin film can be switched by choosing between Pt and Al as the top electrode [5]. The chemical activity (reactive or non-reactive) and the work function of metal electrodes also play important roles in the RS behavior [6–8]. In some oxide materials, the reactive metal (RM) electrode can enhance the endurance performance while the non-reactive metal (NRM) electrode cannot [9–11]. The resistance switching direction can also be altered depending on the activity of the metal electrodes [7,12]. The remarkable effect of the electrode is proposed to arise from interface redox [3], or trapping/de-trapping at the interfacial Schottky junction [13]. Engineering of electrode should be an effective approach to control the functionality of RS devices.

Most of the RS behavior has been reported in polycrystalline thin film so far [1–3,5–7,10,11]. However, some single crystalline thin films are also reported to have excellent RS recently [8,9,14–17]. A comparison between two kinds of films by comparing the presence and absence of grain boundary enlightens us not only about the role of grain boundary but also the role of defect (e.g., oxygen vacancy) in RS behavior. In this letter, we present the investigation of the RS in CeO$_2$ single crystalline thin film by engineering the top electrodes. Oxygen anions/vacancies in CeO$_2$ are very active and have high mobility [18–20]. An electric field can drive redox in CeO$_2$ [21]. CeO$_2$ is an insulator but oxygen vacancies in CeO$_2$ can dope with electrons [22]. The RS behavior in CeO$_2$ is thought to arise from oxygen migration induced redox between conductive CeO$_{2-x}$ and non-conductive CeO$_2$ phase [17]. Here we systematically investigate the RS behavior in the single crystal CeO$_2$ thin films by depositing different kinds of metal electrodes: RM vs. NRM ones. The RS characteristic and retention of resistance state in (Ag, Au, Pt, Al, Ta, Ti)/CeO$_2$/Nb–SrTiO$_3$ heterostructure devices are compared. We have demonstrated that the RS characteristic of RM (i.e., Al, Ta, Ti)/CeO$_2$/Nb–SrTiO$_3$ under the same polarity behaves quite differently from that of NRM (i.e., Ag, Au, Pt)/CeO$_2$/Nb–SrTiO$_3$.

* Corresponding authors. Address: Department of Physics and Astronomy, Louisiana State University, Baton Rouge, LA 70810, USA (D. Chen).
E-mail addresses: zliao1@tigers.lsu.edu (Z. Liao), dmchen@aphy.iphy.ac.cn (D. Chen).

We further show that the RS in NRM/CeO$_2$/Nb–SrTiO$_3$ is volatile while in RM/CeO$_2$/Nb–SrTiO$_3$ is non-volatile. The OFF/ON ratio can be also controlled by selecting top electrode. Therefore, the RS functionality in the devices can be manipulated through electrode engineering.

2. Experiment

The CeO$_2$ single crystalline thin film was epitaxially grown on single crystalline 0.7 wt% Nb-doped SrTiO$_3$(NSTO) (0 0 1) substrate by pulsed laser deposition at 530 °C in oxygen ambient of 15 mTorr. X-ray diffraction (XRD) data shown in Fig. 1a indicates that the grown direction was [1 0 0]. The thickness was 175 nm (see Fig. 1b). High resolution transmission electron microscopy (HRTEM) also confirmed that the film was crystalline and homogeneous (see Fig. 1c and d). The electrodes with different materials were made by magnetron sputtering at room temperature. For each kind of electrode material, an array of 100 μm × 100 μm electrodes, 30 nm thick and with 600 μm separation in both x and y directions, was fabricated on top of the CeO$_2$ thin film by using the standard photolithographic technique. The conductive NSTO substrate was always grounded as the bottom electrode for corresponding characterization. Systematic current–voltage (I–V) sweeping loops $(0 \rightarrow V_{max} \rightarrow -V'_{max} \rightarrow 0)$ were carried out with Keithley 2400 source meter.

3. Results and discussion

Fig. 2 shows the I–V characteristics of six different devices with different types of metal electrodes on the top of the CeO$_2$/NSTO. We could obtain reproducible hysteresis for all kinds of top metal electrodes. Although all six sets of I–V curves exhibit hysteresis and bipolar RS, the devices with NRM (Ag, Au, Pt) as the top electrodes show a different switching direction from that with RM (Al, Ta, Ti) as the top electrodes. In these NRM (Ag, Au, Pt)/CeO$_2$/NSTO devices, resistance is switched from the high resistance state (HRS) to the low resistance state (LRS) with applying positive bias and from LRS to HRS with negative bias, referenced as "*Eightwise*" [14], while RM (Al, Ta, Ti)/CeO$_2$/NSTO ones show a reversed way which behaves like "*Counter Eightwise*" [14]. Although the switching current for the NRM/CeO$_2$/NSTO devices (with small current compliance in

Fig. 2a–c) was much smaller than that used for the RM/CeO$_2$/NSTO ones, the switching behaviors do not change with increasing switching current. Taking Pt/CeO$_2$/NSTO device as an example (as shown in Fig. 3), the I–V sweep curves with different compliance currents (0.1 mA, 1 mA and 10 mA) exhibit the same switching behavior. The bigger compliance current which allows application of bigger bias simply induces bigger OFF/ON ratio. We found that the switching currents in NRM/CeO$_2$/NSTO devices with 10 mA or even100 mA (data not shown) compliance current are comparable with those in RM/CeO$_2$/NSTO ones. These results clearly show the difference of RS behaviors in the devices with RM and NRM electrodes are intrinsic. Thus, different kinds of electrodes regulate different RS directions.

The retention behavior between NRM/CeO$_2$/NSTO and RM/CeO$_2$/NSTO devices displays a remarkable difference too. As shown in Fig. 4a, the consecutive $(0 \rightarrow 2 V \rightarrow 0)$ sweep loops exhibited in Ag/CeO$_2$/NSTO device completely coincide with each other. The time interval between these two sweeps was ~1 s. During the sweep, the initial HRS is switched to LRS under positive bias and the LRS relaxes quickly back to HRS when the electric field is absent, thus the subsequent loop starts from the same resistance state as the previous sweep loop. The sweep loop at the negative bias side also exhibits the same characteristic. This indicates that the RS in NRM/CeO$_2$/NSTO devices is volatile. The switched resistance by the external electric field can relax back to its initial sate quickly. In contrast, the RS in RM/CeO$_2$/NSTO is non-volatile. Taking Al/CeO$_2$/NSTO as an example and shown in Fig. 4b, both HRS and LRS in Al/CeO$_2$/NSTO devices maintain constant without any sign of decay. Therefore, RM electrodes are more applicable than NRM electrodes for practical applications.

A strong rectification effect was observed in both HRS and LRS of NRM/CeO$_2$/NSTO devices (see Fig. 2a–c). In contrast, the I–V curve becomes linear or almost linear at LRS and rectification effect is distinct only at HRS in RM/CeO$_2$/NSTO (see Fig. 2d–f for example). The rectification effect in NRM/CeO$_2$/NSTO devices can be attributed to the presence of Schottky barrier at NRM/CeO$_2$ and CeO$_2$/NSTO junctions. The linear I–V curve observed in the LRS state of RM/CeO$_2$/NSTO devices indicates a qualitative difference of RM/CeO$_2$ and CeO$_2$/NSTO junctions compared to corresponding ones in NRM/CeO$_2$/NSTO devices. The rectification effect could affect the OFF/ON (equal to HRS/LRS) ratio. The HRS/LRS ratio read at 0.24 V for Ta/ and Al/CeO$_2$/NSTO is 770 and 165, respectively, much larger than that of Ti/CeO$_2$/NSTO (HRS/LRS = 4). The smaller OFF/ON ratio of Ti/CeO$_2$/NSTO may be induced by weak rectification effect in both LRS and HRS.

The distinct RS characteristics and retention behaviors between NRM/CeO$_2$/NSTO and RM/CeO$_2$/NSTO devices suggest that the RS mechanisms in these two kinds of devices are completely different. Our previous *in situ* transmission electron microscopy studies have shown direct evidence that the electric field induced migration of oxygen vacancies plays a key role in RS in NRM/CeO$_2$/Pt devices [17]. The electric field will cause a phase transition from CeO$_2$ to CeO$_{2-x}$ due to oxygen migration, enhancing local conductivity in the neighboring CeO$_{2-x}$ phase and creating conductive paths in the oxide. Furthermore, the non-centrosymmetric structure due to the different CeO$_2$/NSTO and NRM/CeO$_2$ interfaces is responsible for the observed "*Eightwise*" RS behavior [17]. It is worth noting that CeO$_2$ is a stable phase while CeO$_{2-x}$ can only be stable at high temperature and/or ultralow pressure. For example, a stable Ce$_2$O$_3$ phase occurs only with the pressure lower than 10^{-95} atm at room temperature [23]. This may help us understand the volatile RS characteristic in NRM/CeO$_2$/NSTO devices. In the absence of an electrical field, the CeO$_{2-x}$ conductive path will be quickly melted resulting from the oxygen infusion into the film even in the vacuum of ~10^{-10} atm [17]. In this study, the NRM/CeO$_2$/NSTO devices were measured at ~1 atm. It is much easier for the conductive Ce$_2$O$_3$ to
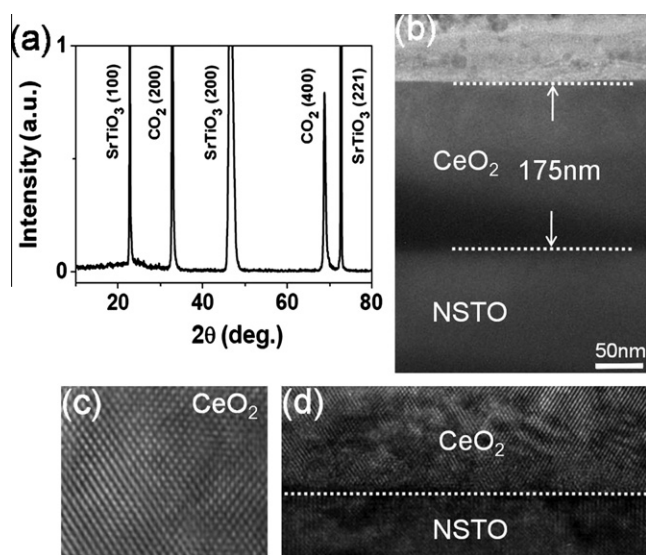
Fig. 1. (a) X-ray diffraction patterns from CeO$_2$/NSTO structure showing growth direction of the film is [1 0 0]. (b) TEM image of CeO$_2$/NSTO cross-section. The surface is flat and thickness of the film is 175 nm. (c) The ZOOM-IN of CeO$_2$ by HRTEM. (d) HRTEM image of CeO$_2$/NSTO interface.
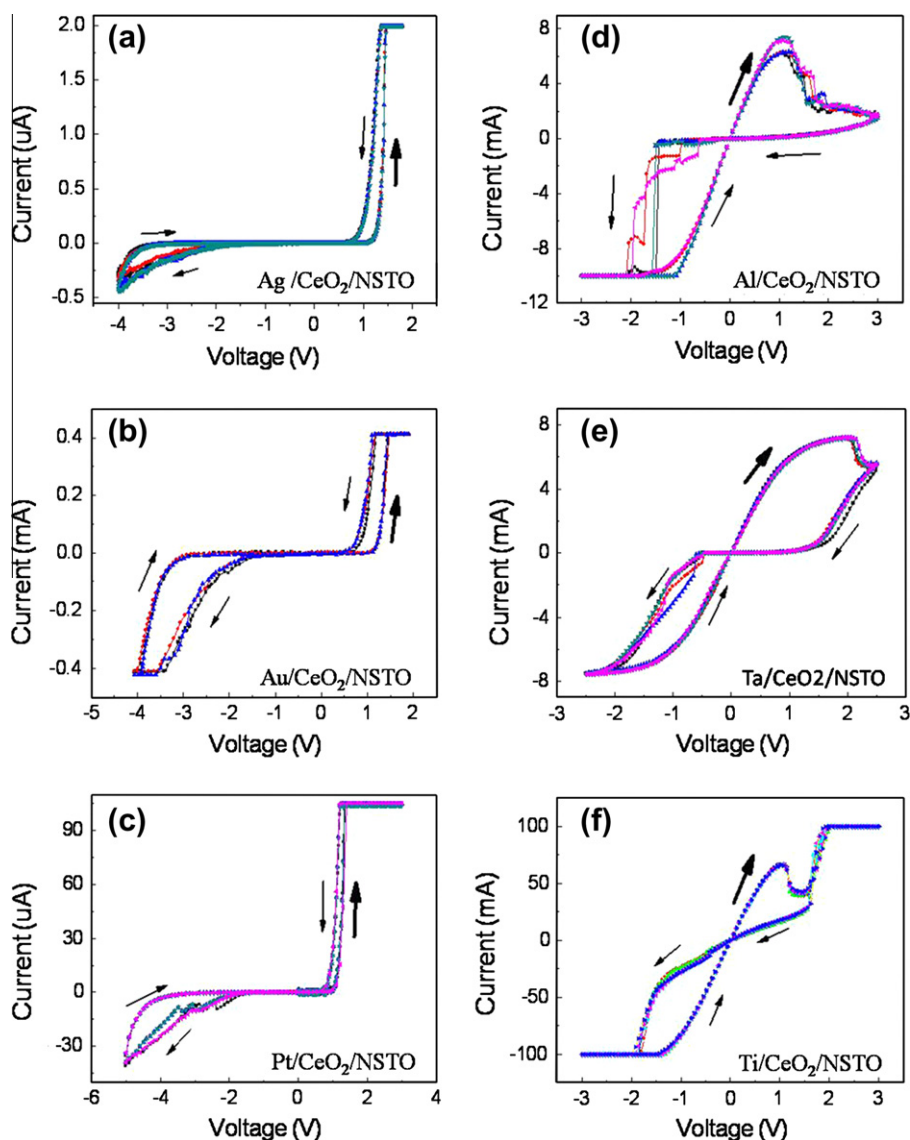
Fig. 2. *I–V* sweep loops $(0 \rightarrow V_{max} \rightarrow -V'_{max} \rightarrow 0)$ of Top-electrode/CeO$_2$/NSTO with different top-electrode materials of Ag, Au, Pt, Al, Ta, Ti. For each kind of top electrode, three consecutive *I–V* sweep loops are shown. Arrows indicate the sweep direction. The *I–V* protocol cycle begins at the thick arrow for this and all figures below.
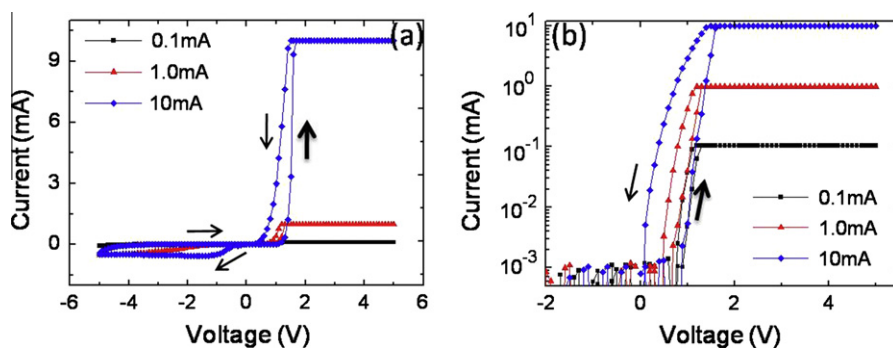

Fig. 3. *I–V* sweep loops $(0 \rightarrow 5 \, V \rightarrow -5 \, V \rightarrow 0)$ of Pt/CeO$_2$/NSTO with different compliance currents. (a) Linear scale; (b) logarithmic scale. Arrows indicate the sweep direction.

recover back to the insulating CeO$_2$ phase, resulting in a volatile RS (see Fig. 4a).

The key to understanding the different RS behavior of the devices with RM electrodes is to realize that, in contrast to NRM electrodes, RM electrodes can easily react with the oxygen to form metal oxide near the interface with CeO$_2$ film. Similar to those observed from PCMO- [7] based devices, the electric field-induced oxygen migration can cause redox at the interface which is suggested to be the main reason for different observed RS [3,7,9–11]. Under the electric field, oxygen will migrate between the top
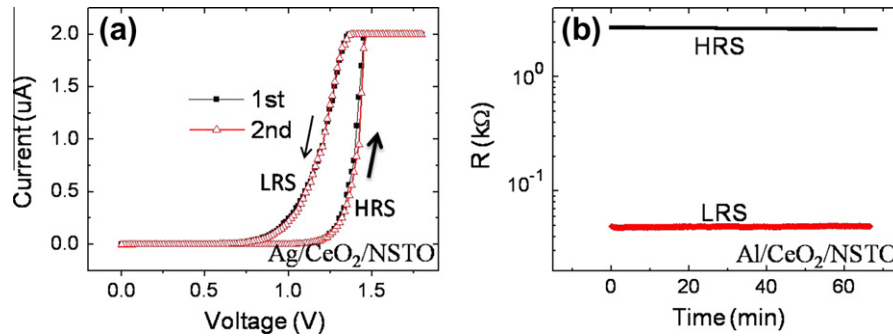
Fig. 4. (a) Consecutive *I*–*V* (0 → 2 V → 0) sweep loops on Ag/CeO$_2$/NSTO. (b) The retention behavior of HRS and LRS of Al/CeO$_2$/NSTO. The resistances were read at 0.3 V. Arrows indicate the sweep direction.

electrode (or top electrode oxide) and metal oxide, depending on the field direction. Under positive bias with respect to the bottom NSTO, oxygen will migrate into the top RM to oxidize it (resulting in HRS) while negative bias can reduce the RM top electrode oxide (resulting in LRS). As a result, RS is "*Counter Eightwise*". In contrast to NRM/CeO$_2$/NSTO, the electrochemical reaction at interface in RM/CeO$_2$/NSTO requires not only migration of oxygen across the interface but also resultant oxidation/reduction. The change of interface's chemical component induced by electrochemical redox will be more stable [3], hence the oxidation/reduction of the RM (Al, Ta, Ti) is stable against thermal fluctuation, thus resulting in excellent retention of RM/CeO$_2$/NSTO devices (see Fig. 4b).

Furthermore, we have found that the RS in the CeO$_2$-based devices is an area-proportional type rather than a filamentary one. To confirm this, we have constructed two kinds of Au electrodes. One is the regular pad with 100 μm × 100 μm contact area with CeO$_2$ films as used for the other experiments of this study. The other one uses a Au-tip (~100 nm × 100 nm contact size) as the electrode as it has been used for TEM characterization [17]. Both setups exhibit the same RS behavior. To test whether the RS is area proportional or filamentary, the LRS between these two setups are compared, since the LRS in the filament model is induced by creation of filaments. The LRS read at 1 V of Au-Pad/CeO$_2$/NSTO with contact area of 100 μm × 100 μm is about 4.7×10^3 Ω, while that for Au-Tip/CeO$_2$/NSTO is 3.5×10^8 Ω. The conductance ratio of LRS of Au-Pad/CeO$_2$/NSTO to Au-Tip/CeO$_2$/NSTO is 10^5, which has same order as the area ratio of two corresponding electrodes, indicating that the RS is proportional to area.

The distinct difference in observed *I*–*V* rectification (see Fig. 2) between RM/CeO$_2$/NSTO and NRM/CeO$_2$/NSTO devices can also be accounted for by the difference of the interface. For NRM electrodes, the NRM/CeO$_2$ is Schottky contact, thus expecting a rectifying *I*–*V* character. For RM electrodes which will reduce CeO$_2$ near the interface, the *I*–*V* rectification of RM/CeO$_2$/NSTO will depends on the relative oxygen concentration level between CeO$_2$ and RM electrodes. At LRS, both CeO$_2$ and top RM oxide accumulate a lot of oxygen vacancies, causing a 'conductive-type' contact and a linear *I*–*V* character. While at HRS, the top RM oxide has less oxygen vacancies than CeO$_2$ film, thus forming a 'Schottky-type' contact and leading to rectifying effect. This scenario is very similar to Metal/TiO$_2$ junction with RM and NRM electrodes [24].

4. Conclusion

In summary, we demonstrated that RS performance in Metal/CeO$_2$/NSTO sandwiched devices strongly depends on the activity of top electrodes. NRM/CeO$_2$/NSTO devices display "*Eightwise*"

bipolar RS, but are volatile with a stable HRS. On the other hand, RM/CeO$_2$/NSTO devices show "*Counter Eightwise*" RS direction and are non-volatile with no sign of decay or relaxation. The devices with RM electrodes also exhibit remarkably different rectification behavior from those with NRM electrodes, due to the difference of electrode/CeO$_2$ interface formation. Among the different RM/CeO$_2$/NSTO devices, Ta/CeO$_2$/NSTO has the biggest OFF/ON ratio. Therefore, the functionality of such RS devices can be manipulated through electrode engineering, enlightening the way to improve performance for technological applications such as resistance random access memory.

Acknowledgements

References

[1] Waser R, Aono M. Nat Mater 2007;6:833.
[2] Sawa A. Mater Today 2008;11:28.
[3] Waser R, Dittmann R, Staikov G, Szot K. Adv Mater 2009;21:2632.
[4] Zhuang WW, Pan W, Ulrich BD, Lee JJ, Stecker L, Burmaster A, et al. Tech Dig Int Electron Devices Meet 2002:193–6.
[5] Do YH, Kwak JS, Bae YC, Jung K, Im H, Hong JP. Thin Solid Films 2010;518:4408.
[6] Lee CB, Kang BS, Benayad A, Lee MJ, Ahn S-E, Kim KH, et al. Appl Phys Lett 2008;93:042115.
[7] Liao ZL, Wang ZZ, Meng Y, Liu ZY, Gao P, Gang JL, et al. Appl Phys Lett 2009;94:253503.
[8] Shibuya K, Dittmann R, Mi S, Waser R. Adv Mater 2010;22:411.
[9] Shen W, Dittmann R, Breuer U, Waser R. Appl Phys Lett 2008;93:222102.
[10] Lv HB, Wang M, Wan HJ, Song YL, Luo WJ, Zhou P, et al. Appl Phys Lett 2009;94:213502.
[11] Yang R, Li XM. Phys Status Solidi A 2011;208:1041–6.
[12] Gang JL, Song SL, Liao ZL, Meng Y, Liang XJ, Dong DM. Chin Phys Lett 2010;27:027301.
[13] Sawa A, Fuji T, Kawasaki M, Tokura Y. Appl Phys Lett 2004;85:4073.
[14] Muenstermann R, Menke T, Dittmann R, Waser R. Adv Mater 2010;22:4819.
[15] Kawai M, Ito K, Shimakawa Y. Appl Phys Lett 2009;95:012109.
[16] Zhang XT, Yu QX, Yao YP, Li XG. Appl Phys Lett 2010;97:222117.
[17] Gao P, Wang ZZ, Fu WY, Liao ZL, Liu KH, Wang WL, et al. Micron 2010;41:301.
[18] Bevan DJM, Kordis J. J Inorg Nucl Chem 1964;26:1509.
[19] Trovarelli A. Catal Rev Sci Eng 1996;38:439.
[20] Mogensen M, Sammes NM, Tompsett GA. Solid State Ionics 2000;12:63.
[21] Gao P, Kang ZC, Fu WY, Wang WL, Bai XD, Wang EG. J Am Chem Soc 2010;132:4197.
[22] Skorodumova NV, Simak SL, Lundqvist BI, Abrikosov IA, Johansson B. Phys Rev Lett 2002;89:166601.
[23] Adachi G, Imanaka N. Chem Rev 1998;98:1479–514.
[24] Yang JJ, Strachan JP, Miao F, Zhang MX, Pickett MD, Yi W, et al. Appl Phys A 2011;102:785–9.